




Calcium and Silicon Precipitation in *Pinus taeda* Needles in Response to Soil Application of Cellulosic Residue

Julierme Zimmer Barbosa¹ 


Evelyn Joslin Mendes² 


Shizuo Maeda³ 

Anne Luiz Sass²

Eloa Araujo⁴ 

Ederlan Magri⁵ 

Stephen Arthur Prior⁶ 

Antonio Carlos Vargas Motta⁷ 

¹Instituto Federal Catarinense, Rio do Sul, SC, Brasil.

²Universidade Federal do Paraná (UFPR), Departamento de Solos e Engenharia Agrícola, Curitiba, PR, Brasil.

³Embrapa Florestas, Colombo PR, Brasil.

⁴Universidade Federal do Paraná (UFPR), Departamento de Solos e Engenharia Agrícola, Curitiba, PR, Brasil.

⁵Universidade Federal do Paraná (UFPR), Curitiba, PR, Brasil.

⁶Agricultural Research Service (USDA), National Soil Dynamics Laboratory, Auburn, AL, USA.

⁷Universidade Federal do Paraná (UFPR), Setor de Ciências Agrárias, Curitiba, PR, Brasil.

Abstract

The use of biosolids as a sustainable alternative in the management of planted *Pinus taeda* forests affects availability of nutrients and beneficial elements. Calcium (Ca) and Silicon (Si) play important roles in plant regulatory and protective systems; therefore, our objective was to use scanning electron microscopy combined with energy-dispersive spectroscopy (SEM–EDS) to analyze the accumulation of elements in *P. taeda* needles grown in soil that received 0 to 60 Mg ha⁻¹ applications of cellulosic waste. Microanalyses of needle sections were performed using a SEM with elemental detection by EDS. Mapping mode allowed for detection and analysis of Ca, Si, and C distributions in needle sections. Calcium and Si precipitation occurred in needles, with Ca accumulating in the phloem and Si in the epidermal cells. Application of 60 Mg ha⁻¹ changed the availability and accumulation of elements, which resulted in more Ca crystals and fewer Si crystals.

Keywords: Calcium oxalate, phytoliths, electron microscopy.

Key message: Different patterns of Ca and Si accumulation (with possible physiological and ecological roles) as function of cellulosic waste application were detected in *P. taeda* by using SEM – EDS microanalysis.

1. INTRODUCTION

World wood demand from planted forests is steadily increasing. In Brazil, planted forests of *Pinus* and *Eucalyptus* have very high productivity levels, with *Pinus taeda* being the most important species in terms of planted forest area in southern Brazil (Oliveira et al., 2018; Dobner and Campoe, 2019). In addition to economic relevance, social and sustainable management practices utilizing organic fertilizers (e.g., biosolid residues from pulp and paper industries) are being implemented as alternatives to promote sustainability of planted forests (Ortega Rodriguez et al., 2018).

Biosolids use can change nutrient dynamics in forest systems and enhanced tree growth (Rodrigues et al., 2023). McLaren et al. (2007) found that biosolids applied to forest soils resulted in substantial build-up of macronutrients and metals in forest litter layers, which changes their availability to plants. For example, the application of residues from recycled paper production increased Ca concentration in *P. taeda* needles, trunks, and roots (Rabel et al., 2020).

Pinus species are highly adapted to acidic soils with poor fertility (Rocha et al., 2019). However, Al toxicity may occur in association with Ca and Mg deficiencies. Silicon, in turn, may play a role in alleviating Al toxicity (Hodson &

Sangster, 1999; Hodson and Evans, 2020). More complex interactions between elements can occur (Hodson & Sangster, 1999; Rocha et al., 2019), and the traditional approach of analyzing needle elemental composition may not be sufficient for understanding physiological changes promoted by different management practices. In addition, elements such as Ca can be found in different forms (i.e., oxalate, sulfate, and carbonate crystals) (Pritchard et al., 2000; He et al., 2012; He et al., 2014; Barbosa et al., 2020; Paiva, 2019).

Calcium crystals can have several functions within plants, such as calcium regulation (storage or excretion), heavy metal detoxification, tissue support, and protection against herbivory (Khan et al., 2023). Silicon can also be found precipitated in plant tissues; amount varies by plant part, plant organ age, and interaction with other elements (Mandlik et al., 2020). Silicon is considered beneficial to plants, mitigating the effects of heavy metals and toxic Al, reducing salt and water stress, and providing protection against herbivory and pathogen infection (Zargar et al., 2019).

Microanalysis techniques have been employed to understand the dynamics of elemental forms and distribution in plant tissues (Dinh et al., 2018; Pongrac et al., 2019; Barbosa et al., 2020; Montanha et al., 2020). These techniques can also be used to deepen knowledge concerning the effects of fertilizer management, toxic substances, and even climate change on plant metabolism and morphology (He et al., 2014; Mandlik et al., 2020).

Research exploring the distribution of elements using microanalysis techniques in *P. taeda* needles is incipient, especially under changing plant nutritional status. Thus, the objective of the present study was to use scanning electron microscopy combined with energy-dispersive spectroscopy (SEM – EDS) to analyze the accumulation of elements in needles of *P. taeda* grown in soil receiving cellulosic waste applications.

2. MATERIAL AND METHODS

2.1. Study site and plant material

Needle samples were collected from a *P. taeda* experimental area located in Pirai do Sul, Paraná state, Brazil (24°24'27.36" S and 49° 58' 34.70" W, altitude of 1102 m). According to Köppen climate classification, the climate of the region is Cfb (Alvares et al., 2013), with annual temperatures varying between 16 and 18°C, and average annual rainfall of 1400 to 1600 mm.

The regional parent material is sandstone and the relief is undulating. Soil in the experimental area was classified as a typic Orthic Quartzarenic Neosol. Analyses of soil physical and chemical attributes were performed to characterize the area (Table 1). For this purpose, soil samples (0-20 cm deep) were dried and ground to pass through a 2 mm sieve. Subsequently, the pH in CaCl₂, potential acidity (H+Al), organic carbon, exchangeable aluminum (Al³⁺), P, K⁺, Ca²⁺, Mg²⁺, and texture were determined following the procedures of Embrapa (2011)

Table 1. Soil characteristic of the experimental area.

pH CaCl ₂	C	Ca ²⁺	Mg ²⁺	K ⁺	Al ³⁺	H+Al	P	Clay	Sand	Silt
	g dm ⁻³	cmol _c dm ⁻³				mg dm ⁻³		g kg ⁻¹		
4,07	3,97	0,04	0,02	0,03	0,69	3,97	0,20	138,0	788,0	74,0

Source: The author.

The experiment consisted of increasing rates of a composted residue (14, 25, 49, and 60 Mg ha⁻¹ of dry material) generated by the cellulose industry. Residue rates were selected to increase soil base saturation by 20, 40, 60, and 80%, respectively. In addition, a control receiving no compost application was included. The residue utilized was a mixture of 70% cellulosic sludge and 30% boiler ash that was composted for ~12 months in the open. *Pinus taeda* seedlings were planted in January 2011 on 2.5 m x 2.5 m spacings. In June of the same year, blocks and experimental plots were laid out; each plot consisted of five rows with five trees per row for a total of 25 trees.

In the present study, we selected representative trees from the control, the 14, and the 60 Mg ha⁻¹ cellulosic sludge treatments. In June 2016, needles were collected randomly from the middle third of three trees per treatment. Samples were stored in coolers for transport to the laboratory. Subsamples were washed with deionized water, dried (60°C), and milled (< 1 mm). Samples were prepared for total N concentration by digestion with sulfuric acid, while K, Ca, Mg, P, S, Fe, Mn, Zn, Cu, and B were determined using inductively coupled plasma (ICP-OES) after nitro-perchloric digestion in a microwave oven (Martins & Reissmann, 2007) (Table 2).

2.2. SEM-EDS

Part of the *P. taeda* needle sample was washed with deionized water, placed on a glass plate, and cut with a stainless-steel blade. Sections (~ 2 mm) from central portions of needles were kept in the dark for 24 h (4 °C) in 3 mL tubes containing 1 mL of FAA fixation solution [formalin 5% (v/v), glacial acetic acid 5% (v/v), and 70% ethanol (v/v)]. Needle sections were then stored in 3 mL tubes containing 1 mL of 70% ethanol until being subjected to dehydration by an ethanol series of 80, 90, 95, and 100% (20 min per step). Needle sections were then subjected to dehydration with liquid CO₂ to a critical point and mounted on aluminum stubs coated with double-sided copper tape.

Microanalyses of needle sections were performed using a SEM (Vega3 LM, Tescan) with elements being detected by EDS (X-MaxN 80 mm², Oxford). The SEM instrument was a thermionic emission system with 3-nm resolution and a tungsten-heated filament as the electron source. Microscope functions were controlled via VegaTC software. The EDS instrument contained an 80 mm² silicon drift detector, and data processing was conducted with AZTech (Advanced) software. Images were obtained with an accelerating voltage of 15 kV in low vacuum. Microanalyses by EDS were conducted with an accelerating voltage of 15 kV, 35° take off angle, and 120 s per image (mapping mode). The mapping mode allowed for the detection and analysis of Ca, Si, and C distribution in needle sections. In the point analysis mode, C, O, Ca, Si, S, and Al were analyzed. These elements were analyzed based on energies and intensities of K- and L-lines and comparison with internal standards (CaSiO₃, SiO₂, ascorbic acid, FeS₂, and Al₂O₃).

3. RESULTS AND DISCUSSION

3.1. Ca precipitation in needles

From photomicrograph images, the following tissues were distinguished in *P. taeda* needle cross sections: mesophyll, epidermis, phloem, and xylem (Figure 1A). Only Ca and Si were accumulated in tissues (Figure 1).

Calcium was detected in all needle tissues (Figure 1D, Figure 1E and Figure 1F), primarily as precipitated crystals in phloem (Figure 2). These Ca precipitates were possibly in the form of Ca oxalate (CaOx) since Ca carbonate would be easily dissolved in an acidic medium (i.e., sample fixation solution). Soil acidity and low soil organic matter could have resulted in low S concentrations in needle tissues (Table 3), which would prevent formation of Ca sulfate crystals. Crystals of CaOx have been observed in various tissues and plant organs, and were formed both in intracellular and extracellular environments (Franceschi & Nakata, 2005; Barbosa et al., 2020; Pongrac et al., 2019).

Occurrence of Ca in phloem increased as a function of cellulosic sludge rate (Figure 2). Twenty-four crystals were counted in the control and 14 Mg ha⁻¹ treatments, while 30 crystals were found in the 60 Mg ha⁻¹ treatment (Table 3); this was possibly due to increased total Ca concentration in needles from the highest treatment (Table 2). The presence of Ca crystals in needles was not expected since the soil concentration was very low. Increases in crystals occurred despite large increases in plant growth, which often results in Ca dilution within tissues (Sass et al., 2020) and increased K and Mg found in tissue (Table 2). The size of the transect cut of needles confirms that enhanced growth had occurred (Figure 2 A, Figure B and Figure C).

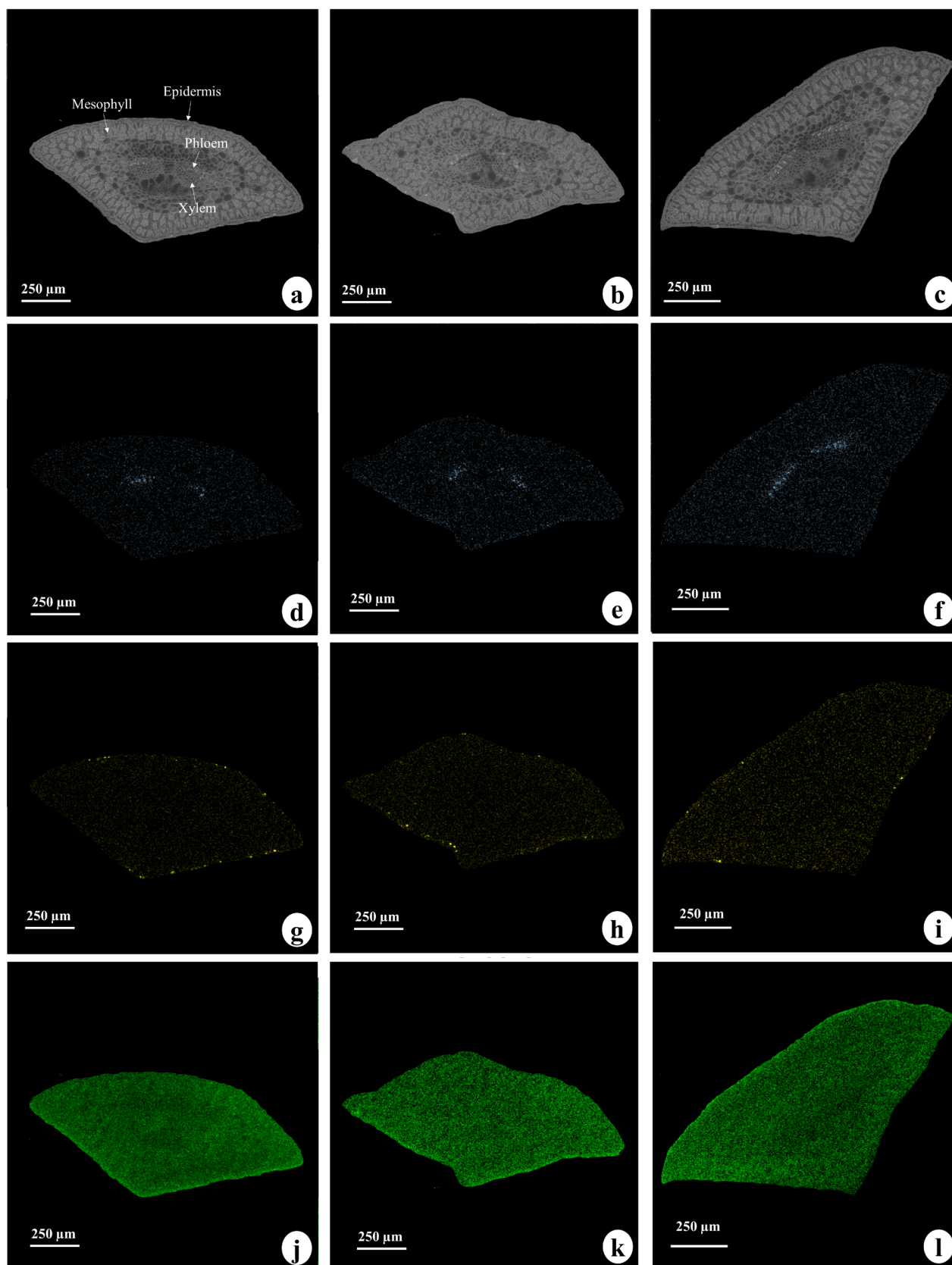


Figure 1. Photomicrograph (a – c) and distribution of Ca (d – f), Si (g – i), and C (j – l) in needles of *Pinus taeda* grown in soil receiving applications of 0 (a, d, g, and j), 14 (b, e, h, and k), and 60 Mg ha⁻¹ (c, f, i, and l) of cellulosic residue. Source: The author.

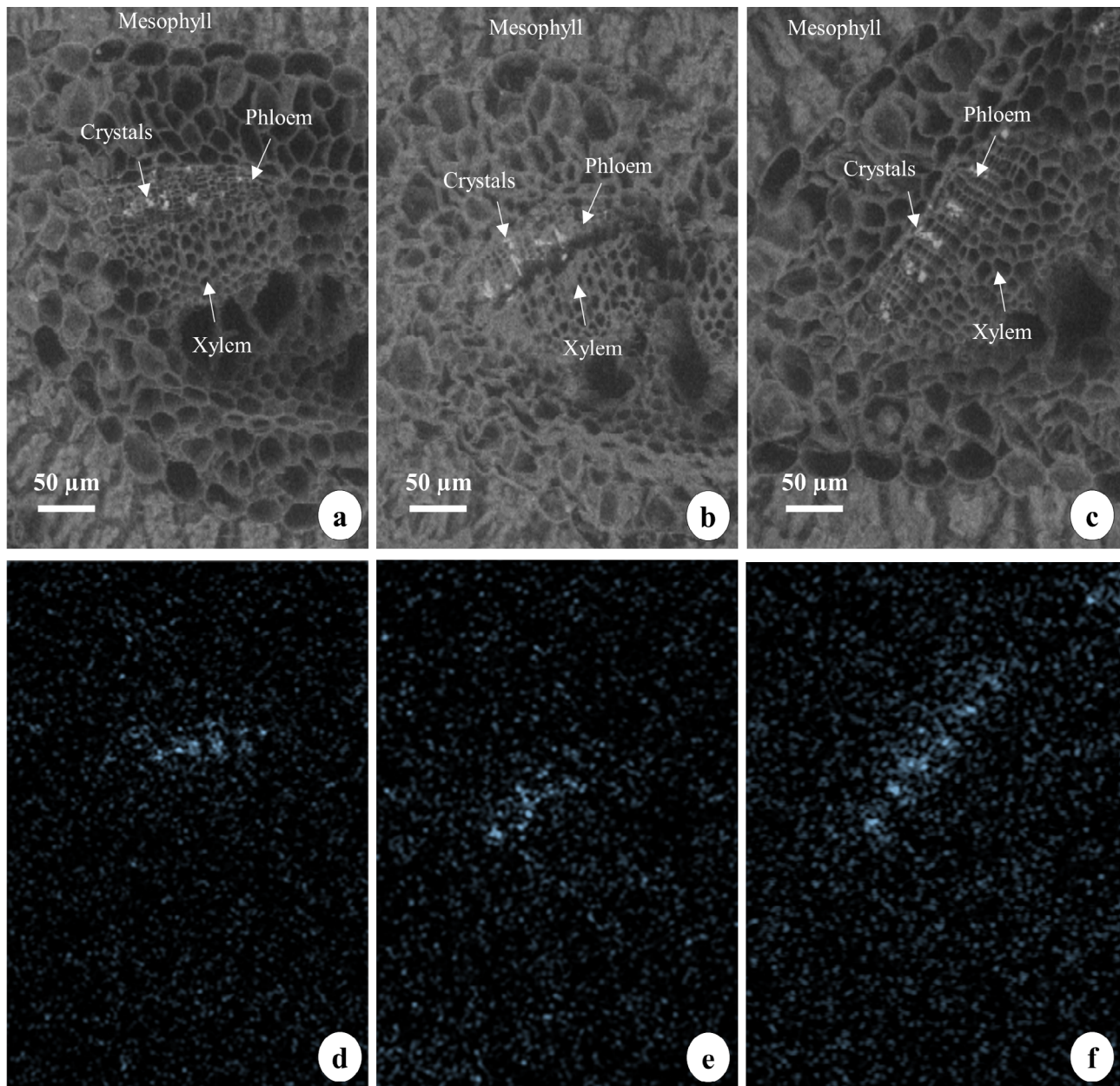


Figure 2. Photomicrograph (a – c) and Ca distribution (d – f) in the vascular bundle region of *Pinus taeda* needles grown in soil receiving applications of 0 (a, d), 14 (b, e), and 60 Mg ha⁻¹ (c, f) of cellulosic waste. Source: The author.

Table 2. Elemental composition of *Pinus taeda* needles as function of cellulosic residue applied to soil in Pirai do Sul, Paraná state, Brazil.

Nutrient	Units	Treatment		
		Control	14 Mg ha ⁻¹	60 Mg ha ⁻¹
N	g kg ⁻¹	15.1±0.5	15.4±0.4	13.9±0.2
K	g kg ⁻¹	4.5±0.5	4.6±0.2	5.5±0.3
Ca	g kg ⁻¹	1.2±0.4	2.9±0.4	2.7±0.4
Mg	g kg ⁻¹	0.3±0.2	0.7±0.1	0.9±0.1
P	g kg ⁻¹	1.4±0.1	1.5±0.2	1.6±0.3
S	g kg ⁻¹	0.8±0.1	0.9±0.1	0.9±0.0
Fe	mg kg ⁻¹	54.2±5.3	62.8±4.0	60.3±9.0
Mn	mg kg ⁻¹	1075±261	877±79	499±98
Zn	mg kg ⁻¹	33.7±6.3	31.1±2.5	25.0±3.0
Cu	mg kg ⁻¹	6.0±0.7	5.5±0.5	5.4±0.3
B	mg kg ⁻¹	13.8±2.6	13.6±1.6	15.5±1.7

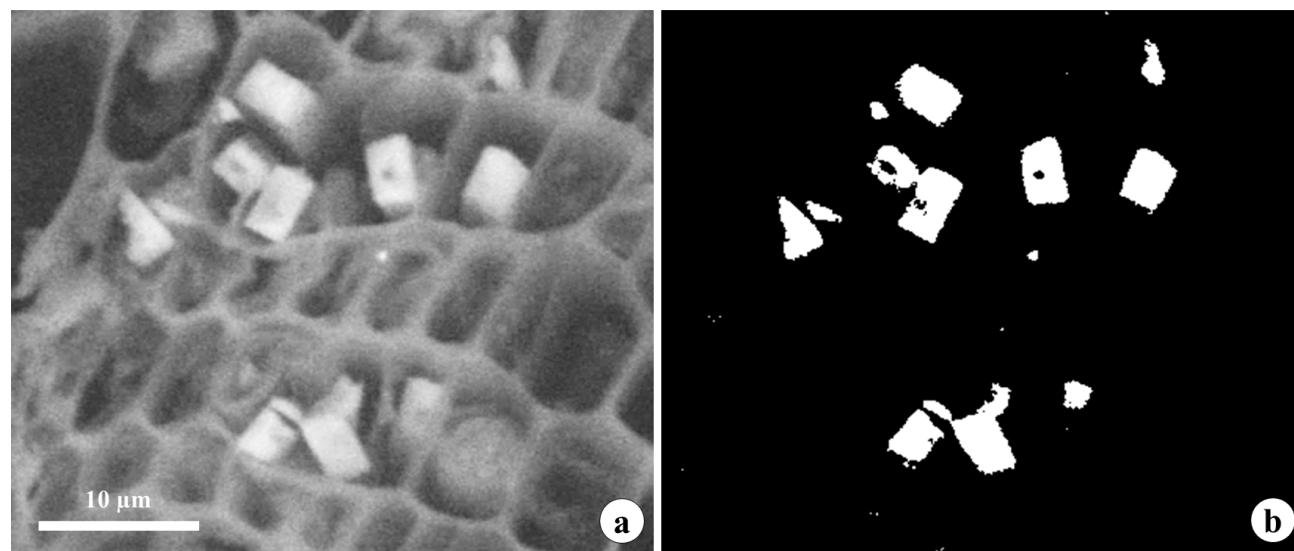
Source: The author.

The formation of CaOx crystals results from biological activity and environmental conditions, and depends on the amount of Ca available to the plant (Weiner and Doeve, 2003; Smith, 2009). Brown et al. (2013) found a positive relationship between the amount of Ca present in leaves of *Acacia phyllodes* and levels of insoluble CaOx; this dynamic was regulated by the concentration of Ca in soil solution.

Potassium deficiency also promotes greater Ca absorption, which led to Ca precipitation in *Araucaria angustifolia* leaves (Barbosa et al., 2017). These crystals act like a Ca storage system, regulating Ca stocks in plant tissue (Franceschi & Nakata, 2005; Karabourniotis et al., 2020). Under Ca deficient conditions, dissociation of CaOx crystals can result in remobilization of Ca (Volk et al., 2002; Turpault et al., 2019).

Pinus taeda normally has two annual needle flushes (in some cases, three) (Motta et al., 2014). We hypothesize that, when plants are not in the flush phase, it is possible that increased Ca levels in phloem provides for the formation of CaOx crystals; this may be especially true if increased amounts of Ca are available in soil. Calcium is very immobile in plants and a pivotal structural component of cell walls (Hawkesford et al., 2012). However, formation of crystals related to Ca regulation and stocks in plant tissues may be a consequence of high Ca levels in phloem of *P. taeda* needles from high rates of cellulosic sludge application (Figure 2). Specific studies are required to expand knowledge on Ca dynamics in phloem tissue during *P. taeda* needle flush development.

Phloem crystals were prismatic in nature (Figure 3). There were five morphological variations of CaOx crystals based on shape: druse, needle, styloid, sand crystals, and prismatic (Pierantoni, 2019). Extracellular crystals are generally rhombohedral or prismatic in shape, while crystals formed in intracellular spaces can present any of the habits mentioned above (Franceschi & Nakata, 2005).

**Figure 3.** Details of Ca crystals found in the phloem of *Pinus taeda* needles cultivated in soil receiving cellulosic waste. a – Normal photomicrograph; b – Black and white photomicrograph. Source: The author.

According to He et al. (2012), prismatic crystals are typically five to ten μm in length, and are associated with phloem fibrous cells, or cells associated with them. Up to 50% of cells of specific tissues had one or two crystals. Crystals of CaOx can occur inside vacuoles (usually in a cell specialized in crystal formation), or in the apoplast (associated with the cell wall) (Franceschi & Nakata, 2005). Fink (1991) evaluated the presence of crystals in needles of several conifer species. In *Pinus* spp., intracellular crystals are preferentially formed in the phloem, and rarely extracellular crystals are formed in the mesophyll. This indicates that Pinaceae species are more evolved than other conifer species, since only extracellular crystals have been found in Araucariaceae, Taxodiaceae, and Taxaceae (Fink, 1991).

In addition to Ca regulation, the formation of crystals containing Ca in plants can perform several other functions such as detoxification of metals, harnessing light, and protection against herbivore attack (Franceschi and Nakata, 2005; Karabourniotis et al., 2020). Since Ca crystals did not occur near or on the surface of needles, they were likely not related to luminosity. Although the low Al concentrations detected in crystals (Table 3) could affect Al dynamics, it is important to assess whether increases in Al availability would increase this element in crystals.

The main function generally conferred to calcium crystals is Ca storage and regulation (Khan et al., 2023), with druses being the main crystal form related to this function (Nakata, 2003). However, depending on crystal shape, they can perform different functions within the plant (Lawrie et al., 2023). Druses and prismatic crystals can improve photosynthesis by remitting light and making better use by photosynthetic cells (Gal et al., 2012; Pierantoni et al., 2017), suggesting a possible function of these forms found in needles (Figure 3). Raphides, which were not found in *Pinus* needles in this experiment (in addition to regulating calcium storage), are the main form responsible for providing plant defense against herbivores (Nakata, 2003; Paiva, 2021).

Table 3. Number of crystals and percentage of Ca, C, and O in crystals formed in the phloem of *Pinus taeda* needles in response to application of cellulosic residue to soil.

Treatment	Mean \pm sd	Maximum	Minimum
Number			
Control	24 \pm 5	28	18
14 Mg ha ⁻¹	24 \pm 12	37	14
60 Mg ha ⁻¹	30 \pm 9	40	24

Table 3. Continued

Treatment	Mean \pm sd	Maximum	Minimum
Ca (%)			
Control	4.1 \pm 0.9	5.9	2.9
14 Mg ha ⁻¹	3.6 \pm 0.9	4.7	2.5
60 Mg ha ⁻¹	3.7 \pm 0.5	4.5	2.8
C (%)			
Control	62 \pm 2	65	58
14 Mg ha ⁻¹	63 \pm 3	69	60
60 Mg ha ⁻¹	63 \pm 1	65	61
O (%)			
Control	34 \pm 2	39	31
14 Mg ha ⁻¹	33 \pm 2	37	29
60 Mg ha ⁻¹	33 \pm 2	36	30
Al (%)			
Control	0.04 \pm 0.01	0.06	0.03
14 Mg ha ⁻¹	0.07 \pm 0.03	0.10	0.04
60 Mg ha ⁻¹	0.06 \pm 0.04	0.12	0.00
S (%)			
Control	0.05 \pm 0.01	0.06	0.04
14 Mg ha ⁻¹	0.05 \pm 0.01	0.06	0.04
60 Mg ha ⁻¹	0.04 \pm 0.01	0.06	0.04

Source: The author.

3.2. Si precipitation in needles

Silicon was present in all tissues, with preferential accumulation in the epidermis in the absence of cellulosic residue (Figure 1G, Figure 1H, Figure 1I – I and Figure 4). Silicon is considered a beneficial element for plants, affecting several mechanisms of protection and mitigation of abiotic and biotic stresses (Luyckx et al., 2017; Broadley et al., 2012). This element is absorbed by roots, transported via transpiration flow, and accumulates in aerial plant parts, usually in epidermal tissues (Barbosa et al., 2020; Guerriero et al., 2020).

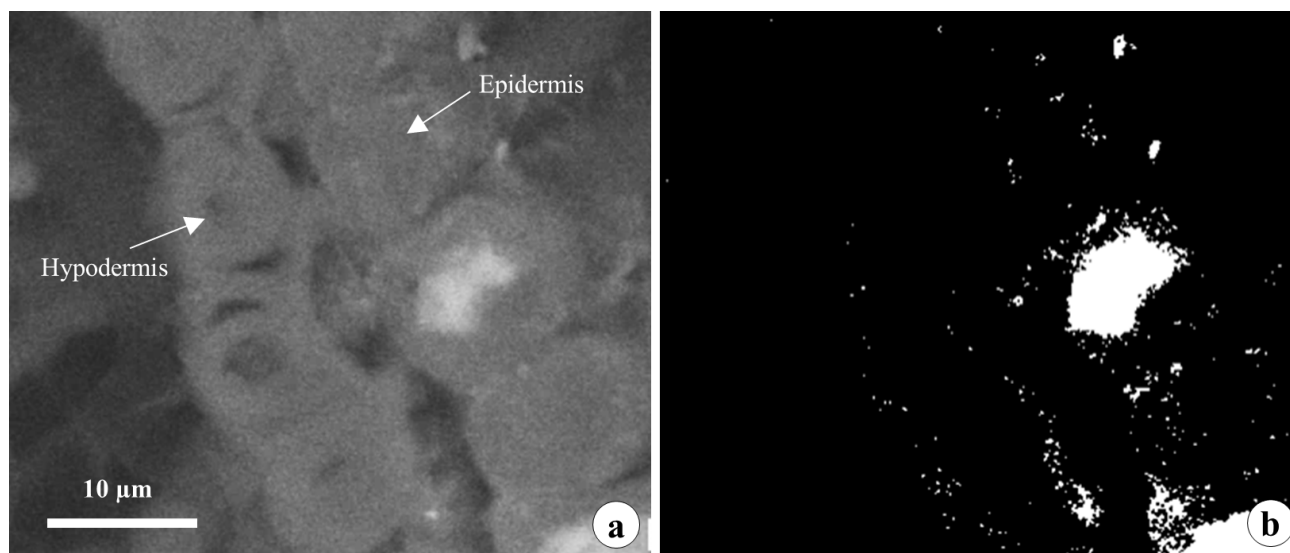


Figure 4. Details of Si crystals found in the epidermis of *Pinus taeda* needles cultivated in soil receiving cellulosic waste. a – Normal photomicrograph; b – Black and white photomicrograph. Source: The author.

Preferential accumulation of Si in the form of precipitates occurred throughout the epidermis of *P. taeda* needles (Figure 1 G, Figure 1H, Figure 1I and Figure 4). Deposition can be quite diverse, whether in the form of precipitates inside the cells or as amorphous material impregnating the middle lamella of cell walls in the epidermis, stomata, mesophyll, and tracheids (Sangster et al., 1997; Mvondo-She and Marais, 2019; Barbosa et al., 2020). Analyzing needles from 12 *Pinus* species, Sangster et al. (1997) found that four species showed accumulation in tracheids (*P. koraiensis*, *P. parviflora*, *P. peuce*, and *P. strobus* “radiata”), and three displayed accumulation in isolated epidermal cells (*P. cooperi*, *P. strobus* “radiata”, and *P. sylvestris*). Contrary to observations of Hodson and Sangster (2002) and Niemiec et al. (2017) for *P. strobus*, at this work we did not observed Al accumulation in needles, likely due to low Al concentration in plant tissue (Table 4).

The control treatment had 19 Si crystals, while the 14 and 60 Mg ha⁻¹ treatments had 18 and 13 crystals, respectively (Table 4). Greater tree growth was favored by the 14 Mg ha⁻¹ cellulosic residue application, with little increase observed at 20 Mg ha⁻¹ to 60 Mg ha⁻¹ (Sass et al., 2020). Thus, increasing cellulosic residue application rate probably diluted Si concentration in needles and consequently decreased amount of Si precipitates. Species belonging to gymnosperms are considered low Si accumulators; this genetic factor may also have influenced the low amount of Si precipitated in needles (Zargar et al., 2019).

Table 4. Number of crystals and percentage of Si, C, and O in crystals formed in the epidermis of *Pinus taeda* needles in response to application of cellulosic residue to soil.

Treatment	Mean±sd	Maximum	Minimum
Number			
Control	19±2	21	17
14 Mg ha ⁻¹	18±1	19	17
60 Mg ha ⁻¹	13±1	14	13
Si (%)			
Control	4.4±0.5	5	4.1
14 Mg ha ⁻¹	4.0±0.3	4.2	3.8
60 Mg ha ⁻¹	4.0±0.6	4.5	3.9
C (%)			
Control	63±3	65	60
14 Mg ha ⁻¹	66±2	68	65
60 Mg ha ⁻¹	65±3	66	60
O (%)			
Control	32±2	35	30
14 Mg ha ⁻¹	29±1	30	28
60 Mg ha ⁻¹	30±2	34	29
Al (%)			
Control	0.06±0	0.06	0.06
14 Mg ha ⁻¹	n.d.	n.d.	n.d.
60 Mg ha ⁻¹	0.03±0	0.03	0.03
S (%)			
Control	0.03±0	0.03	0.03
14 Mg ha ⁻¹	0.03±0.01	0.04	0.03
60 Mg ha ⁻¹	0.02±0	0.02	0.02

n.d. denotes not detected.

Source: The author

Silicon accumulation in plant tissue promotes greater resistance to attack by fungi and herbivores when Si precipitation occurs in the epidermis (Mandlik et al., 2020; Broadley et al., 2012). Thus, Si precipitation in the epidermis of *P. taeda* may contribute to increased tolerance of pests (especially insects). If Si precipitation occurred in isolated cells in the epidermis, a null effect against fungal infection would be expected. However, further studies are required to broaden our knowledge regarding the ecological and physiological interactions associated with Si precipitation in *P. taeda*.


4. CONCLUSIONS

The use of SEM – EDS microanalysis illustrated different patterns of elemental accumulation that may have possible physiological and ecological roles in *P. taeda*. Calcium and Si precipitation occurred in needles of *P. taeda*, with Ca accumulating in the phloem, while Si accumulated in epidermal cells. Application of 14 Mg ha⁻¹ of cellulosic sludge did not affect precipitation of these elements compared to the control treatment. However, with the application of 60 Mg ha⁻¹, Ca crystals tended to be formed in the phloem, and the number of Si crystals in needle epidermal tissue decreased; changes were probably due to variations in the availability and absorption of these elements. Analysis of crystal composition did not indicate significant changes in concentrations of Ca and Si.

SUBMISSION STATUS

Received: 28 Nov. 2024

Accepted: 02 Aug. 2025

Associate editor: Marcos Pereira 

CORRESPONDENCE TO

Evelyn Joslin Mendes

R. dos Funcionários, 1540, CEP 80035-050, Curitiba, PR, Brasil
e-mail: evelynjmendes@gmail.com

AUTHORS' CONTRIBUTIONS

Julierme Zimmer Barbosa: Conceptualization (Equal), Data curation (Equal), Methodology (Equal), Writing - original draft (Equal), Writing - review & editing (Equal).

Evelyn Joslin Mendes: Writing - original draft (Equal), Writing - review & editing (Equal).

Shizuo Maeda: Writing - original draft (Equal).

Anne Luiz Sass: Data curation (Equal), Methodology (Equal), Writing - original draft (Equal).

Eloa Araujo: Writing - original draft (Equal).

Ederlan Magri: Data curation (Equal), Methodology (Equal), Writing - original draft (Equal).

Stephen Arthur Prior: Writing - original draft (Equal), Writing - review & editing (Equal).

Antonio Carlos Vargas Motta: Conceptualization (Equal), Funding acquisition (Equal), Writing - original draft (Equal).

DATA AVAILABILITY

Data not available.

FINANCIAL SUPPORT

The authors thank the CMPC Florestal companies and Embrapa Floresta for field work support and Center of Electronic Microscopy of the Federal University of Paraná (CME-UFPR) for microscopy analysis. Antônio Carlos Vargas Motta is grateful to the National Council for Scientific and Technological Development (CNPq) for financial support (project n° 314834/2023-0) and to the Coordination for the Improvement of Higher Education Personnel (CAPES) for scholarship support.

REFERENCES

- Alvares CA, Stape JL, Sentelhas PC, et al. Köppen's climate classification map for Brazil. *Meteorol Zeitschrift* 2013; 22:711–728. <https://doi.org/10.1127/0941-2948/2013/0507>
- Barbosa JZ, Constantino V, Zanette F, et al. Soil fertility affects elemental distribution in needles of the conifer *Araucaria angustifolia*: a microanalytical study. *CERNE* 2017; 23:257–266. <https://doi.org/10.1590/0104776020172302313>
- Barbosa JZ, Motta AC V, Reis AR dos, et al. Spatial distribution of structural elements in leaves of *Ilex paraguariensis*: physiological and ecological implications. *Trees* 2020; 34:101–110. <https://doi.org/10.1007/s00468-019-01900-y>
- Broadley M, Brown P, Cakmak I, et al. Marschner's Mineral Nutrition of Higher Plants. Elsevier. 2012; 249–269
- Brown SL, Warwick NWM, Prychid CJ. Does aridity influence the morphology, distribution and accumulation of calcium oxalate crystals in *Acacia* (Leguminosae: Mimosoideae)? *Plant Physiology and Biochemistry* 2013; 73:219–228. <https://doi.org/10.1016/j.plaphy.2013.10.006>
- Oliveira RK, Higa AR, Silva LD, et al. Emergy-based sustainability assessment of a loblolly pine (*Pinus taeda*) production system in southern Brazil. *Ecological Indicators* 2018; 93:481–489. <https://doi.org/10.1016/j.ecolind.2018.05.027>
- Dinh N, van Der Ent A, Mulligan DR, Nguyen AV. Zinc and lead accumulation characteristics and in vivo distribution of Zn²⁺ in the hyperaccumulator *Noccaea caerulea* elucidated with fluorescent probes and laser confocal microscopy. *Environmental and Experimental Botany* 2018; 147:1–12. <https://doi.org/10.1016/j.envexpbot.2017.10.008>
- Dobner M, Campoe OC. Meteorological effects on 30-years-grown *Pinus taeda* under a gradient of crown thinning intensities in southern Brazil. *Forest Ecology and Management* 2019; 453:117624. <https://doi.org/10.1016/j.foreco.2019.117624>

- Embrapa. Manual de Métodos de Análise de Solo, 2nd edn. Embrapa Solos, Rio de Janeiro; 2011
- Fink S. Comparative microscopical studies on the patterns of calcium oxalate distribution in the needles of various conifer species. *Botanica Acta* 2019; 104:306–315. <https://doi.org/10.1111/j.1438-8677.1991.tb00235.x>
- Franceschi VR, Nakata PA. Calcium oxalate in plants: formation and function. *Annual Review of Plant Biology* 2005; 56:41–71. <https://doi.org/10.1146/annurev.arplant.56.032604.144106>
- Gal A, Brumfeld V, Weiner S, Addadi L, Oron, D. Certain biominerals in leaves function as light scatterers. *Advanced Materials* 2012; 24(10):OP77–OP83. <https://doi.org/10.1002/adma.201104548>
- Guerriero G, Stokes I, Valle N, et al. Visualising silicon in plants: histochemistry, silica sculptures and elemental imaging. *Cells* 2020; 9:1066. <https://doi.org/10.3390/cells9041066>
- Hawkesford M, Horst W, Kichey T, et al. *Marschner's Mineral Nutrition of Higher Plants*. Elsevier. 2012; 135–189
- He H, Bleby TM, Veneklaas EJ, et al. Morphologies and elemental compositions of calcium crystals in phylloides and branchlets of *Acacia roborum* (Leguminosae: Mimosoideae). *Annals of Botany* 2012; 109:887–896. <https://doi.org/10.1093/aob/mcs004>
- He H, Veneklaas EJ, Kuo J, Lambers H. Physiological and ecological significance of biomineralization in plants. *Trends in Plant Science* 2014; 19(3):166–174. <https://doi.org/10.1016/j.tplants.2013.11.002>
- Hodson MJ, Sangster AG. Aluminium/silicon interactions in conifers. *Journal of Inorganic Biochemistry* 1999; 76:89–98. [https://doi.org/10.1016/S0162-0134\(99\)00119-1](https://doi.org/10.1016/S0162-0134(99)00119-1)
- Hodson MJ, Sangster AG. X-ray microanalytical studies of mineral localization in the needles of white pine (*Pinus strobus* L.). *Annals of Botany* 2002; 89:367–374. <https://doi.org/10.1093/aob/mcf052>
- Hodson MJ, Evans DE. Aluminium-silicon interactions in higher plants: an update. *Journal of Experimental Botany* 2020. 71(21):6719–6729. <https://doi.org/10.1093/jxb/eraa024>
- Karabourniotis G, Horner HT, Bresta P, Nikolopoulos D, Liakopoulos G. New insights into the functions of carbon-calcium inclusions in plants. *New Phytologist* 2020; 228(30):845–854. <https://doi.org/10.1111/nph.16763>
- Khan MI, Pandith SA, Shah MA, Reshi ZA. Calcium oxalate crystals, the plant 'Gemstones': insights into their synthesis and physiological implications in plants. *Plant and Cell Physiology*. 2023; 64(10):1124–1138. <https://doi.org/10.1093/pcp/pcad081>
- Lawrie NS, Cueto NM, Sini F, Salam AG, Ding H, Vancolen A, Nelson JM, Erkens RHJ, Perversi G. Systematic review on raphide morphotype calcium oxalate crystals in angiosperms. *AoB Plants* 2023; 15(4):1–16. <https://doi.org/10.1093/aobpla/plad031>
- Luyckx M, Lutts S, Hausman JF, Guerriero G. Silicon and plants: current knowledge and technological perspectives. *Frontiers in Plant Science* 2017; 23(8):411. <https://doi.org/10.3389/fpls.2017.00411>
- Mandlik R, Thakral V, Raturi G, Shinde S, Nikolić M, Tripathi DK, Sonah H, Deshmukh R. Significance of silicon uptake, transport, and deposition in plants. *Journal of Experimental Botany* 2020; 71:6703–6718. <https://doi.org/10.1093/jxb/eraa301>
- Martins APL, Reissmann CB. Material vegetal e as rotinas laboratoriais nos procedimentos químicos-analíticos. *Scientia Agraria* 2007; 8:1. <https://doi.org/105380/rsa.v8il.8336>
- McLaren RG, Clucas LM, Speir TW, van Schaik AP. Distribution and movement of nutrients and metals in a *Pinus radiata* forest soil following applications of biosolids. *Environmental Pollution* 2007; 147:32–40. <https://doi.org/10.1016/j.envpol.2006.08.027>
- Montanha GS, Rodrigues ES, Marques JPR, De Almeida E, Dos Reis A R, Pereira de Carvalho H W. X-ray fluorescence spectroscopy (XRF) applied to plant science: challenges towards *in vivo* analysis of plants. *Metallomics* 2020; 12(2):183–192. <https://doi.org/10.1039/c9mt00237e>
- Motta ACV, Barbosa JZ, Consalter R, Reissmann CB. Nutrição e adubação da cultura de Pinus. In: Prado RM, Wadt PGS (eds) *Nutrição e adubação de espécies florestais e palmeiras*, 1st edn. FUNEP. Jaboticabal. 2014; 383–426
- Mvondo-She MA, Marais D. The investigation of silicon localization and accumulation in citrus. *Plants* 2019; 8:200. <https://doi.org/10.3390/plants8070200>
- Nakata PA. Advances in our understanding of calcium oxalate crystal formation and function in plants. *Plant Science* 2003; 164(6):901–909. [https://doi.org/10.1016/S0168-9452\(03\)00120-1](https://doi.org/10.1016/S0168-9452(03)00120-1)
- Niemiec M, Chowaniak M, Paluch Ł. Accumulation of chromium, aluminum, barium and arsenic in selected elements of a forest ecosystem in the Przedbabiogórskie Mountain Range in the Western Carpathians. *Journal of Elementology* 2017; 22(3). <https://bibliotekanauki.pl/articles/958262.pdf>
- Ortega Rodriguez DR, Andrade G de C, Bellote AFJ, Tomazello-Filho. Effect of pulp and paper mill sludge on the development of 17-year-old loblolly pine (*Pinus taeda* L.) trees in Southern Brazil. *Forest Ecology Management* 2018; 422:179–189. <https://doi.org/10.1016/j.foreco.2018.04.016>
- Paiva ÉAS. Are calcium oxalate crystals a dynamic calcium store in plants? *New Phytologist* 2019; 223:1707–1711. <https://doi.org/10.1111/nph.15912>
- Pierantoni M. Functions and Properties of Calcium Oxalate, Calcium Carbonate and Silica Deposits in Leaves. The Weizmann Institute of Science. 2019. <https://doi.org/10.34933/wis.000486>
- Pierantoni M, Tenne R, Brumfeld V, Kiss V, Oron D, Addadi L, Weiner S. Plants and light manipulation: the integrated mineral system in okra leaves. *Advanced Science* 2017; 4(5):1600416. <https://doi.org/10.1002/advs.201600416>
- Pongrac P, Baltreñaite E, Vavpetic P, et al. Tissue-specific element profiles in Scots pine (*pinus sylvestris* L.) needles. *Trees* 2019; 33:91–101. <https://doi.org/10.1007/s00468-018-1761-5>
- Pritchard SG, Prior SA, Rogers HH, Peterson CM. Calcium sulfate deposits associated with needle substomatal cavities of container grown longleaf pine (*Pinus palustris*). *International Journal of Plant Science* 2000; 161(6):917–923. <https://doi.org/10.1086/317560>
- Rabel D de O, Maeda S, Araujo EM, et al. Recycled alkaline paper waste influenced growth and structure of *Pinus taeda* L. forest. *New Forests* 2020; 52:249–270. <https://doi.org/10.1007/s11056-020-09791-5>
- Rocha JHT, du Toit B, Gonçalves JL de M. Ca and Mg nutrition and its application in *Eucalyptus* and *Pinus* plantations. *For Ecol Manage* 2019; 442:63–78. <https://doi.org/10.1016/j.foreco.2019.03.062>
- Rodrigues VDS, Motta ACV, Barbosa JZ, Ercole TM, Prior SA. Wood production and nutritional status of *Pinus taeda* L. in response to fertilization and liming: a meta-analysis of the Americas. *iForest-Biogeosciences and Forestry* 2023; 16(4):195–201. <https://doi.org/10.3832/ifer4296-016>

- Mandlik R, Thakral V, Raturi G, Shinde S, Nikolić M, Tripathi DK, Sonah H, Deshmukh R. Significance of silicon uptake, transport, and deposition in plants. *Journal of Experimental Botany* 2020; 71(21):6703–6718. <https://doi.org/10.1093/jxb/eraa301>
- Sangster AG, Williams SE, Hodson MJ. Silica deposition in the needles of the Gymnosperms. II Scanning electron microscopy and X-ray microanalysis. In: Pinilla A, Juan-Tresserras J, Machado MJ (eds) *The State-of-the-Art of Phytoliths in Soils and Plants*. Centro de Ciencias Medioambientales, Madrid. 1997; 135–146
- Sass AL, Bassaco MVM, Motta ACV, Maeda S, Barbosa JZ, Bognola IA, et al. Cellulosic industrial waste to enhance *Pinus taeda* nutrition and growth: a study in subtropical Brazil. *Scientia Florestalis* 2020; 48(126):e3165. <https://doi.org/10.18671/scifor.v48n126.1>
- Smith KT, Shortle WC, Connolly JH, Minocha R, Jellison J. Calcium fertilization increases the concentration of calcium in sapwood and calcium oxalate in foliage of red spruce. *Environmental and Experimental Botany* 2009; 67:277–283. <https://doi.org/10.1016/j.envexpbot.2009.07.007>
- Turpault MP, Calvaruso C, Dincher M, et al. Contribution of carbonates and oxalates to the calcium cycle in three beech temperate forest ecosystems with contrasting soil calcium availability. *Biogeochemistry* 2019; 146:51–70. <https://doi.org/10.1007/s10533-019-00610-4>
- Volk GM, Lynch-Holm VJ, Kostman TA, et al. The role of druse and raphide calcium oxalate crystals in tissue calcium regulation in *Pistia stratiotes* leaves. *Plant Biol* 2002; 4:34–45. <https://doi.org/10.1055/s-2002-20434>
- Weiner S, Dove PM. An overview of biomineralization processes and the problem of the vital effect. *Rev Mineral Geochemistry* 2003; 54:1–29. <https://doi.org/10.2113/0540001>
- Zargar SM, Mahajan R, Bhat JA, et al. Role of silicon in plant stress tolerance: opportunities to achieve a sustainable cropping system. *3 Biotech* 2019; 9:73. <https://doi.org/10.1007/s13205-019-1613-z>